

Validation of the numerical stress intensity factor calculation of surface cracks using crack propagation experiments

J. Lebahn, H. Heyer, M. Sander

University of Rostock, Institute of Structural Mechanics, Albert-Einstein-Str. 2, 18059 Rostock, Germany

jens.lebahn@uni-rostock.de, horst.heyer@uni-rostock.de, manuela.sander@uni-rostock.de

ABSTRACT. *This paper deals with the numerical calculation of stress intensity factors (SIF) of surface cracks under Mode I conditions and its validation by crack propagation experiments on round bars with cyclic tension and bending loading. The SIFs were calculated numerically from energy release rate by use of the MVCCI-method. In order to determine the SIFs for the intersection point an extrapolation is used. Furthermore the intersection points' singularity of the stress field and the area of influence were investigated numerically on single edge notched specimens with varying crack geometries. It was possible to validate the numerical calculation of SIFs and to deduce guidelines for the extrapolation. Moreover, the crack propagation experiments were used to check the crack geometry and to investigate there dependencies e.g. of stress ratio and overloads. As has been proved semi-elliptical crack geometries appear independent of the stress ratio and overloads as long as the assumptions of the linear elastic fracture mechanics are fulfilled. Also, the crack front intersects the surface in a certain angle where the $1/\sqrt{r}$ -singularity of the stress field is nearly fulfilled.*

INTRODUCTION

Efficient residual lifetime calculation of cracked structures can be done by analytical crack propagation simulations. The knowledge of the crack path and the related solution of the stress intensity factor (SIF) is a basic requirement for the simulation. In order to achieve SIFs numerical simulations are performed e.g. by use of the Finite Element Method. Uncertainties of the calculated SIFs result from the methods character as an approximation solution and the specific feature of the crack front surface point.

In literature [1, 4, 7, 11] it is well known that the $1/\sqrt{r}$ -singularity of the stress field at the intersection point of the crack front and the structure surface is not fulfilled in general whereby the conventional SIF loses its availability. Pook [4] has shown that the stress fields singularity λ_σ depends on the Poisson's ratio ν and the angle β between the crack front and the surface of the structure. E.g. for an angle $\beta = 90^\circ$ and a Poisson's ratio $\nu = 0,3$ Benthem [1] calculated analytically a singularity λ_σ of -0,452. Furthermore

Pook [4] stated and other authors [7, 9] almost attested numerically and experimentally for plane surfaces the existence of an certain angle β_s

$$\beta_s = \arctan\left(\frac{v-2}{v}\right) \quad (1)$$

where the $1/\sqrt{r}$ -singularity of the stress field is fulfilled. Heyder [7] even pointed out that for naturally curved crack fronts all points of the crack front satisfy the $1/\sqrt{r}$ -singularity. Furthermore Hutar et al. [11] estimate the influence of the intersection points area of middle tension specimens by numerical simulation. He pointed out for $v = 0,3$ that the surface influence on the singularity of the stress field decays in a distance to the surface of about 20 % of the half specimen thickness.

In order to determine SIFs for the intersection point some authors [6, 14] make use of an extrapolation. Thereby the SIFs in some distance from the surface are fitted by e.g. a quadratic polynomial function [6]. This function was fitted e.g. by Shin and Cai [6] to the SIFs which ranges from 20 – 100% of the half crack front length.

A basic assumption for the analytical crack propagation simulation is that the crack front exhibits an elliptical geometry. Serveral authors [2, 5, 8] have attested the development of elliptical crack fronts by crack propagation tests. However, in the numerical crack propagation simulations performed by Hou [12] deviations from the elliptical form are reported and explained by the crack closure effect.

Crack propagation experiments on round bars

The crack propagation tests were performed on smooth round steel (34CrNiMo6) bars with a diameter of 20 mm. The specimens were loaded by cyclic tension or bending with constant amplitude. To investigate the development of the crack geometry beach marks, which were generated by single overloads, were measured under a traveling microscope. To initiate a crack the specimens were notched by micro bore holes, Figure 1. The crack length was measured using the DC potential drop method. The required calibration curve was obtained from pretests.

Table 1 gives an overview of the variants of the performed crack propagation tests. It should be noted that a dye was used for the tests with an overload ratio of 1 to deduce paint marks alternative to the beach marks.

Table 1. Overview of the performed crack propagation experiments

Stress ratio	Overload ratio = 1,8		Overload ratio = 1	
	Bending	Tension	Bending	Tension
-1	-	4	-	-
0,1	18	6	-	3
0,5	2	-	-	-

The analysis of the crack fronts include the measuring of the beach marks, black curves in Figure 1, and check their elliptical form by fitting ellipse, red curves, to them. In some tests the beach marks deviate from the elliptical form, see Figure 1 b. It could be observed that these deviations were caused by very high overloads which lead to large plastic zones especially in the surface region of the crack front. Therefore a retardation of the crack propagation occurs in the surface region. The size of the plastic zones were estimated by FE simulations and showed a good agreement with analytical models. So the numerical investigations from Hou [12] could be confirmed. For all further tests a limit for the maximum SIF $K_{\max} < 2.000 \text{ N/mm}^{3/2}$ was applied.

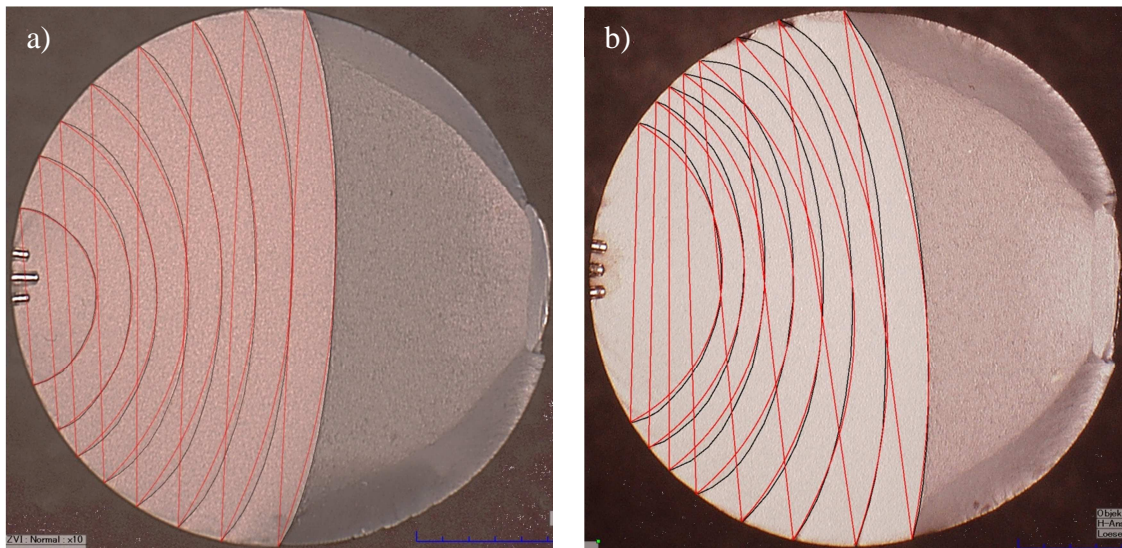


Figure 1. Crack fronts with beach marks (black) and ellipse (red): a) nearly elliptical formed beach marks, b) deviations from the elliptical form

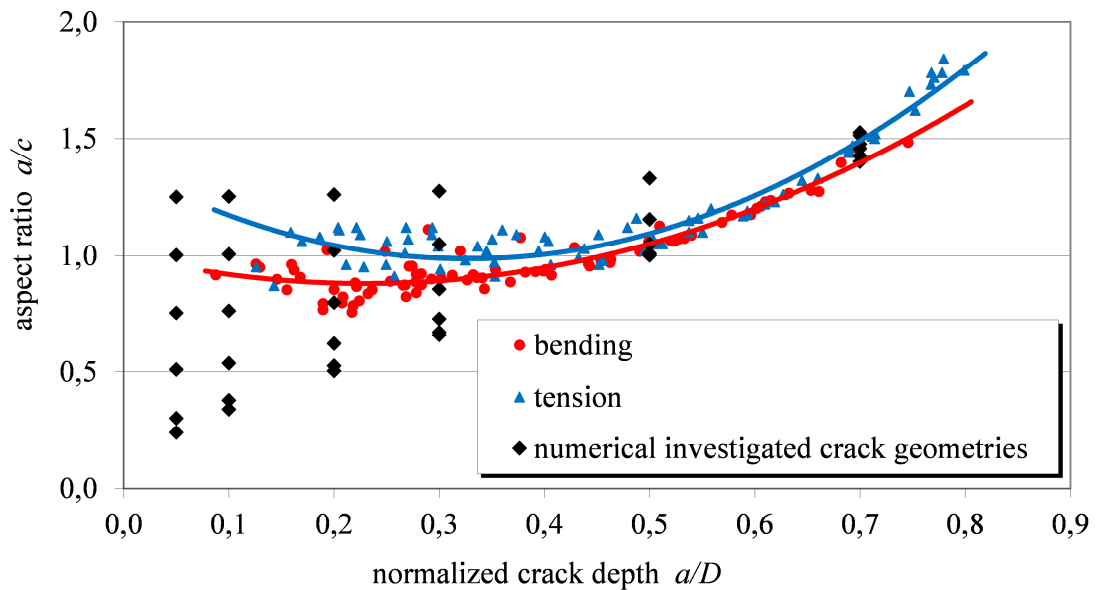


Figure 2. Crack front geometries of all beach marks and SIF solution

The main result of the crack propagation experiments is the development of the crack geometry. In Figure 2 the aspect ratio of the beach marks are shown over the crack depth. It can be observed that the development of the crack geometry depends on the type of loading. Moreover it can be ascertained that the development of the crack geometry is independent of stress ratio and overload ratio.

Also the angle between the crack front and the surface of the structure at the intersection point is investigated experimentally, Figure 3. It becomes obvious that the angles exhibit a linear dependence of the crack depth. The analytical value for plane surfaces calculated by Eq. (1) amounts about 100°. The mean value of all angles exceeds the analytical value about 8%. The development of the intersection angles is almost the same for tension and bending loading. Also plotted in Figure 3 is the deviation between numerically calculated and extrapolated SIF solutions for $a/D = 0,1$. As can be seen, the deviations increase for crack fronts which differ from the naturally crack front obtained from the crack propagation tests.

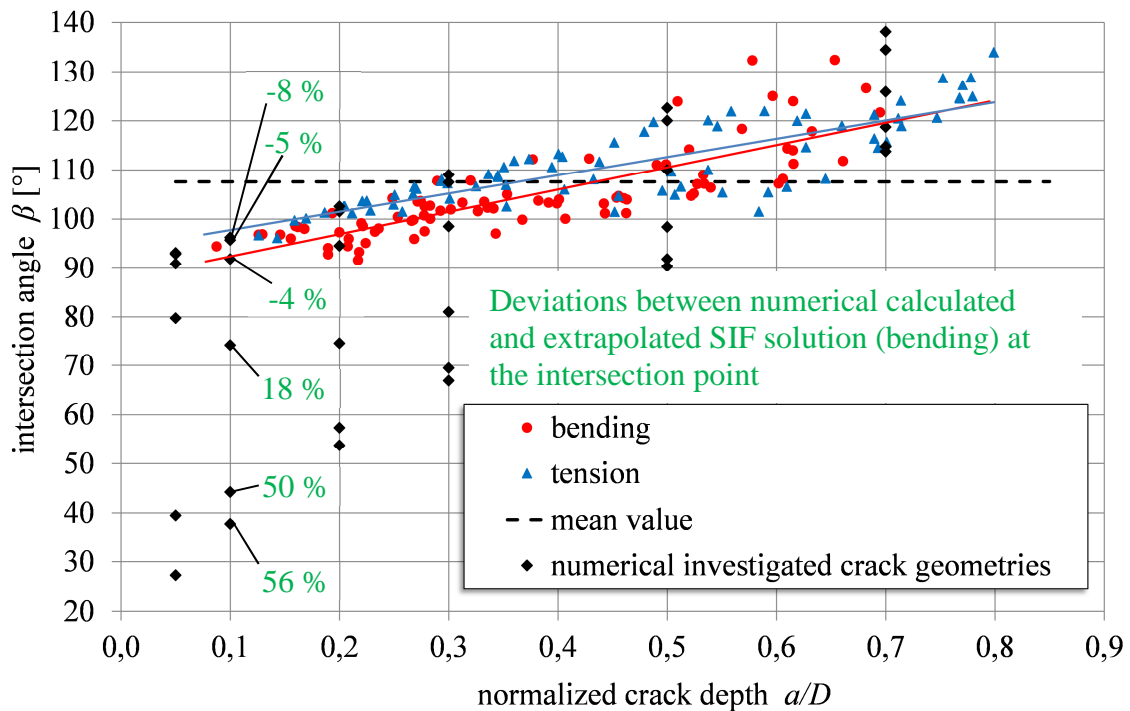


Figure 3. Crack front angle at the intersection point of all beach marks and crack geometries from SIF solution

Numerical Investigations

The SIFs for Mode I were calculated from energy release rates

$$K^2 = G \cdot E' \quad \text{with} \quad E' = \begin{cases} E & \text{plane stress} \\ E/(1-\nu^2) & \text{plane strain} \end{cases} \quad (2)$$

by use of the plane strain conditions. E is the elastic modulus and ν the Poisson's ratio. As mentioned, the SIF at the intersection point was calculated by an extrapolation of the SIF along the crack front, see the next chapter. The numerical calculation of the energy release rates were performed with the FE-software MSC Marc/Mentat 2007 by use of the MVCCI-method [3, 10]. For the discretization linear hexaeder elements were used. The special requirements of the mesh for the use of the MVCCI-method are investigated in [14]. After this the element size near the crack front was set about $a/20$. Also double symmetry was used, see Figure 4.

In addition to the crack propagation tests numerical investigations of the thickness of the boundary layer effect were performed to deduce guidelines for the extrapolation. These investigations were carried out on a standard compact tension specimen (CT) with a thickness of $t = 10$ mm using three-dimensional finite element simulations, Figure 5 a). A crack with $a = 27,5$ mm and a straight crack front is assumed, Figure 5 b). Thus the ratio of crack length to width of the specimen a/w amounts to 0,38.

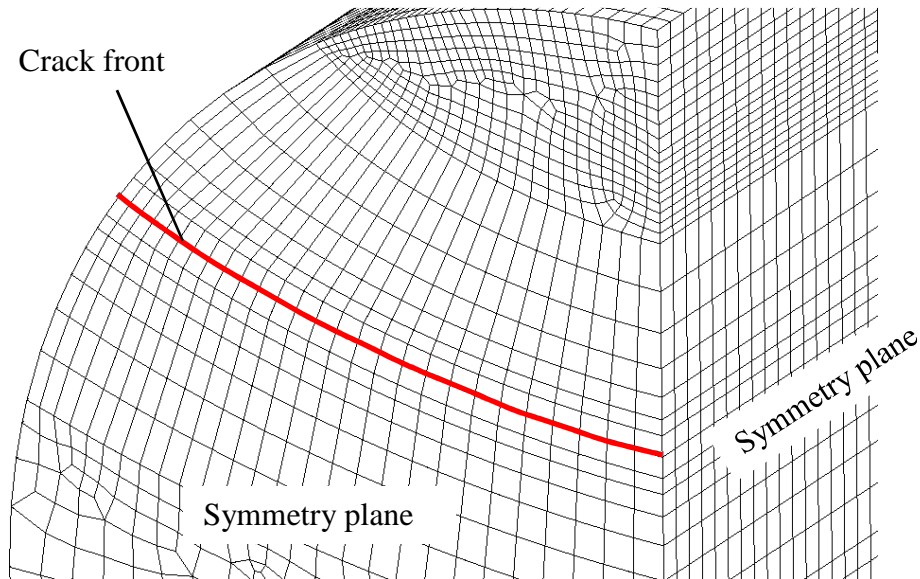


Figure 4. FE- mesh of a round bar with crack by utilization of double symmetry

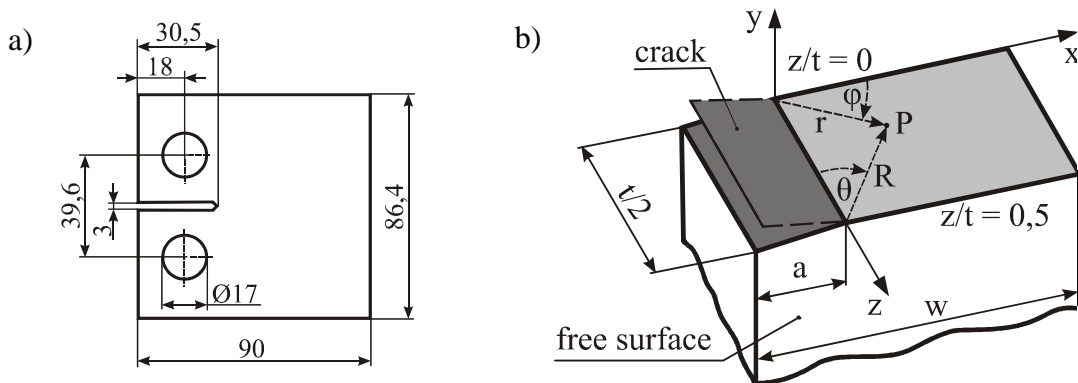


Figure 5. a) CT-specimen, b) Definition of the crack front geometry

Due to the symmetry only one-quarter of the specimen is meshed with twenty-node isoparametric elements. Near the crack front up to a distance of $r = 0,5$ mm and within a layer thickness of 0,5 mm near the free surface a very fine mesh with an element size of 0,01 mm is used. Towards the middle plane of the specimen with $z/t = 0$ the element size is gradually increased in through-thickness direction up to a size of 0,1 mm. The FE-simulations are carried out under the assumption of a linear-elastic material law with $E = 210.000$ MPa and $\nu = 0,3$.

The displacement field near the crack front can be written as superposition of two terms

$$u_{ij} = A_{ij}(\varphi, z) \cdot r^{0,5} + B_{ij}(\varphi, \theta) \cdot R^\lambda \quad (3)$$

based on the known cylindrical singularity for the stresses inside the body and an unknown vertex singularity in spherical coordinates with the exponent λ independent of z [14]. The FE-analyses are evaluated with regard to the crack face displacements in y -direction in a cylindrical coordinate system. For every plane ($z/t = \text{const.}$) these displacements in the vicinity of the crack front ($\varphi = 180^\circ$) can be expressed as follows:

$$u(r) = C \cdot r^{\lambda_u} + D \cdot r^{\lambda_u+1}. \quad (4)$$

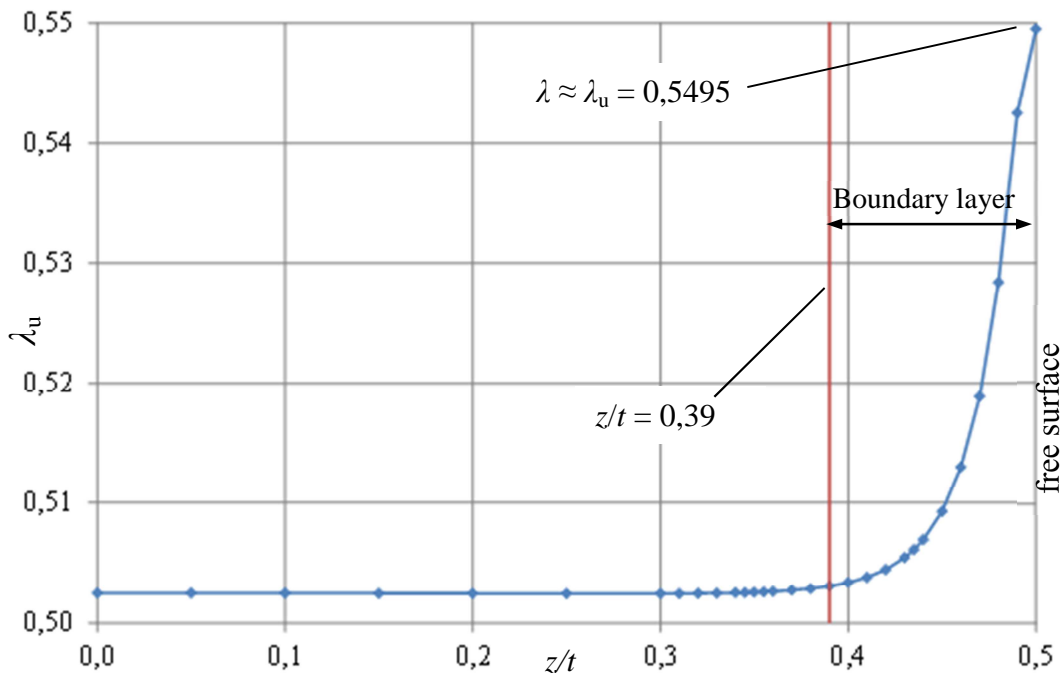


Figure 6. Influence of the vertex singularity λ on the exponent λ_u for different layers

For the numerical evaluation of the exponent λ_u it is advantageous to consider an additional second term of higher order in Eq. (4). In the free surface the exponent λ_u is equal the vertex singularity exponent λ and tends towards 0,5 in the middle plane of the specimen where the second term of Eq. (3) becomes zero. The thickness of the boundary layer influenced by the vertex singularity is defined as the region near the free surface in which λ_u differs from the classical value 0,5. The exponent λ_u is determined in

different layers $0 \leq z/t \leq 0,5$ after Eq. (4) by a regression analysis with the program MATLAB from the computed displacements in a range of $0,02 \text{ mm} \leq r \leq 1,225 \text{ mm}$. The exponent varies along the specimen thickness being close to 0,5 ($\lambda_u = 0,5025$) in the middle plane of the model, Figure 6. This is considered as a sufficient agreement with the theoretical value. In the free surface the value of the exponent is $\lambda_u = 0,5495$. The associated exponent $\lambda_\sigma = \lambda_u - 1 = -0,4505$ is in very good agreement with the theoretical value from Benthem [1]. For a layer $z/t \leq 0,39$ the influence of the vertex singularity λ on the exponent λ_u is almost decayed, Figure 6. So the boundary layer thickness is about 22 % of the half specimen thickness which is in good accordance to Hutar et al. [11].

Validation of the numerical SIF calculation

The validation of the SIF calculation occurs by analytical crack propagation simulations of the tests. Therefore the software NASGRO 6.02 was used. The required SIF solution for tension and bending includes six crack depths reaching from $0,05 \leq a/D \leq 0,7$ and six aspect ratios reaching from $0,1 \leq a/b \leq 1,25$ with b being the half axes of the elliptical crack. The SIFs have been calculated for the deepest point and the surface point of the crack front and entered in NASGRO. After defining of an initial crack geometry the crack propagation for bending and tension loading is calculated by NASGRO depending on the SIF solution. As an initial crack depth $a/D = 0,05$ was chosen with the related aspect ratio deduced from the crack propagation tests, Figure 2.

As mentioned an extrapolation is used to derive the SIFs at the intersection point. Therefore a polynomial function is fitted through the SIF in a special area of the crack front. The parameters of the extrapolation are the order p (2, 3, 4) of the polynomial function as well as the beginning δ and ending ε of the regression area. The beginning varies from $0 \leq \delta \leq 0,3$ the ending from $0,3 \leq \varepsilon \leq 1$ of the half crack fronts' normalized arc length. For all combinations of the 3 parameters analytical crack propagation simulations were performed. Furthermore the deviations between the a/D - a/c -curve from the analytical crack propagation simulation and the beach marks were calculated to find the optimum parameters of the extrapolation.

It could be observed that all parameter combinations lead to aspect ratios in the analytical crack propagation simulation which are smaller than those from the crack propagation tests. By multiplying the SIFs at the intersection point with a value μ between $0,9 \leq \mu \leq 0,95$ the agreement between simulation and test increases. For $\mu = 0,95$ the development of the crack geometry of the simulation is shown in Figure 7 for bending and tension loading. On the one hand the extrapolation which leads to the minimum deviations between simulation and experiment was used for the SIF calculation of the intersection point and on the other hand the direct numerical values were used. It is obvious that the extrapolation leads to a better accordance between simulation and experiment. The parameters of the optimum extrapolation are: $p = 2$, $\delta = 0,275$ and $\varepsilon = 1$. So the parameters are in good agreement with those from Shin and Cai [6]. Furthermore the regression area is independent of the boundary layer effect which decays about 22 % from the surface, as could be proved numerically.

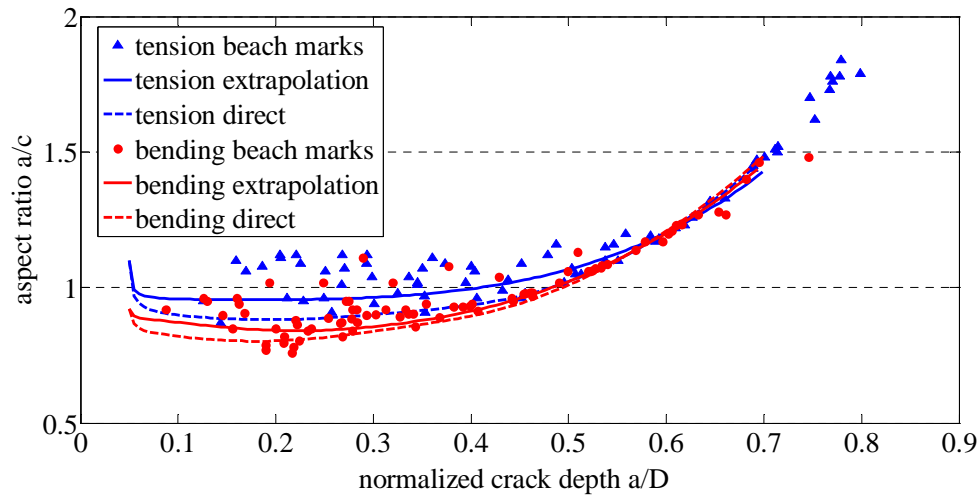


Figure 7. Development of crack geometry from experiment and simulation

Conclusion

The crack propagation tests showed the formation of semi-elliptical surface cracks, which crack geometry depends on load type and is independent of stress ratio and overload ratio. The results demonstrate that intersection angles are not constant for curved surfaces as it is observed for plane surfaces. The crack propagation test could be used for the validation of the numerical SIF calculation. Based on analytical crack propagation simulations of the tests and the numerical investigations concerning the boundary layer thickness guidelines for the extrapolation of the SIF at the intersection point were deduced.

REFERENCES

1. Benthem, J. P. (1977) *Int. J. of Solids* **13**, 479 – 492
2. Müller, H. M.; Müller, S.; Munz, D.; Newman, J. (1986) *Frac. Mech.* **17**, ASTM STP 905, Philadelphia, 625 – 643
3. Shivakumar, K.N.; Tan, P. W.; Newman, J. C. (1988) *Int. J. Fract.* **36**, 43 – 50
4. Pook, L. P. (1994) *Eng. Frac. Mech.* **48**, 367 – 378
5. Lin, X. B.; Smith, R. A. (1997) *Int. J. of Fatigue* **19**, 461 – 469
6. Shin, C. S.; Cai, C. Q. (2004) *Int. J. of Frac.* **129**, 239 – 264
7. Heyder, M.; Kolk, K.; Kuhn, G. (2005) *Eng. Frac. Mech.* **72**, 2095 – 2105
8. Lütkepohl, K.; Esderts, A. (2007) *DVM-Bericht* **239**, Berlin, 23 – 32
9. Branco, R.; Antunes, F. V. (2008) *Eng. Frac. Mech.* **75**, 3020 – 3037
10. Buchholz, F.-G. (2008) In: *DVM-Bericht* **240**, Berlin, 163 – 174
11. Hutar, P.; Náhlík, L. (2008) *Applied and Computational Mech.* **2**, 45 – 52
12. Hou, C.-Y. (2008) *Int. J. of Fatigue* **30**, 1036 – 1046
13. De Matos, P.F.P.; Nowell, D. (2008) *Int. J. of Fatigue* **30**, 1930 – 1943
14. Müller, T.; Heyer, H.; Sander, M. (2011) *DVM-Bericht* **243**, Berlin, 55 - 64